Homochiral Oligopeptides by Chiral Amplification within Two-Dimensional Crystalline Self-Assemblies at the Air–Water Interface; Relevance to Biomolecular Handedness

Isabelle Weissbuch,*[a] Helmut Zepik,[a] Gérard Bolbach,[b] Edna Shavit,[a] Mao Tang,[a] Torben R. Jensen,[c] Kristian Kjaer,[c] Leslie Leiserowitz,*[a] and Meir Lahav*[a]

Abstract: A possible role that might have been played by ordered clusters at interfaces for the generation of homochiral oligopeptides under prebiotic conditions has been probed by a catalyzed polymerization of amphiphilic activated α-amino acids, in racemic and chiral non-racemic forms, which had self-assembled into two-dimensional (2D) ordered crystallites at the air–aqueous solution interface. As model systems we studied N^{ε}-stearoyl-lysine thioethyl ester (C_{18}-TE-Lys), γ-stearyl-glutamic thioethyl ester (C_{18}-TE-Glu), N^{α}-carboxyanhydride of γ-stearyl-glutamic acid (C_{18}-Glu NCA) and γ-stearyl-glutamic thioacid (C_{18}-thio-Glu). According to in-situ grazing incidence X-ray diffraction measurements on the water surface, (*R*,*S*)-C_{18}-TE-Lys, (*R*,*S*)-C_{18}-TE-Glu, and (*R*,*S*)-C_{18}-Glu-NCA amphiphiles self-assembled into ordered racemic 2D crystallites. Oligopeptides 2–12 units long were obtained at the air–aqueous solution interface after injection of appropriate catalysts into the water subphase. The experimental relative abundance of oligopeptides with homochiral sequence generated from (*R*,*S*)-C_{18}-TE-Lys and (*R*,*S*)-C_{18}-TE-Glu, as determined by mass spectrometry on enantioselectively deuterium-labeled samples, was found to be significantly larger than that obtained from (*R*,*S*) C_{18}-thio-Glu which polymerizes randomly. An efficient chiral amplification was obtained in the polymerization of *non*-racemic mixtures of C_{18}-Glu-NCA since the monomer molecules in the racemic 2D crystallites are oriented such that the reaction occurs between heterochiral molecules related by glide symmetry to yield heterochiral oligopeptides whereas the enantiomer in excess, in the enantiomorphous crystallites, yield oligopeptides of a single handedness.

Keywords: chiral amplification · peptides · polymerization · self-assembly · X-ray diffraction

Introduction

The biopolymers of life are built from chiral molecules of a single handedness: the proteins from *S*-α-amino acid building blocks and the nucleic acids from *R*-sugars. One of the unsolved puzzles of the origin of life is related to the transition from prebiotic racemic chemistry to chiral biology.[1–3] Chiral non-racemic mixtures of α-amino acids have been generated from racemates by spontaneous symmetry breaking processes such as stochastic crystallization,[4–6] or by induced enantioselective destruction upon irradiation with circularly polarized light.[1] An open question still remains as to how homochiral oligopeptides of a single handedness might have been generated from such mixtures of low enantiomeric imbalance.[3, 7–16] Polymerization of racemic mixtures of monomers in solution[17–19] is expected to yield polymers comprising a random sequence of left- and right-handed repeat units following a binomial distribution, although recently it has been reported that polymerization of racemic N^{α}-carboxyanhydrides of hydrophobic α-amino acids in buffered aqueous solutions has been found to yield an enhanced abundance of homochiral oligopeptides.[20, 21]

Grazing incidence X-ray diffraction (GIXD) studies have demonstrated that a large variety of amphiphilic molecules self-assemble, at the air–water interface, into two-dimensional (2D) crystalline domains, of structures that can be determined at the molecular level.[22] Two-dimensional self-assemblies formed on the water surface can provide ideal systems for stereospecific and enantioselective chemical reactions.[23–30] The 2D assemblies promote effective molecular ordering, yet allow substantial molecular flexibility and

[a] Dr. I. Weissbuch, Prof. Dr. L. Leiserowitz, Prof. Dr. M. Lahav, Dr. H. Zepik, E. Shavit, M. Tang
Department of Materials and Interfaces
The Weizmann Institute of Science, 76100-Rehovot (Israel)
Fax: (+972) 89-34-4138
E-mail: isabelle.weissbuch@weizmann.ac.il
leslie.leiserowitz@weizmann.ac.il
meir.lahav@weizmann.ac.il

[b] Dr. G. Bolbach
Laboratoire de Chimie Structurale Organique et Biologique
Université Pierre et Marie Curie, 75252 Paris Cedex 05 (France)

[c] Dr. T. R. Jensen, Dr. K. Kjaer
Materials Research Department
Risø National Laboratory, 4000 Roskilde (Denmark)

0947-6539/03/0908-1782 $ 20.00+.50/0

further afford access of catalysts from the aqueous subphase to the ordered, flexible molecules. Thus, based on a process involving self-assembly followed by lattice-controlled polymerization reaction, we propose a general scenario for the generation of homochiral oligopeptides of a single handedness from non-racemic mixtures of activated α-amino acid derivatives.[31]

By analogy to 3D crystals, racemic mixtures of amphiphilic molecules at interfaces self-assemble into 2D crystallites of three types: 1) racemic compounds in which both enantiomers are packed together, related to one another by glide symmetry;[32] 2) enantiomorphous conglomerates involving segregation of the enantiomers, and 3) enantiomerically disordered solid solutions.

Here we focus on chiral non-racemic mixtures that undergo a phase separation by self-assembly into a 2D racemic crystalline phase and an enantiomorphous 2D phase of the enantiomer in excess (Scheme 1).[33] The chemical properties

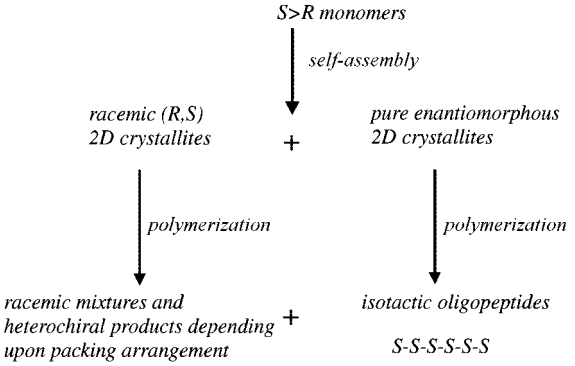

Scheme 1. A chiral amplification process of oligopeptides starting from non-racemic mixtures of monomers undergoing phase separation by self-assembly at the air–water interface.

of each crystalline phase should be substantially different, yielding products that differ in composition as well as in the length of the oligomers. Polymerization within the enantiomorphous crystallites would yield homochiral oligopeptides of a single handedness, whereas reaction within the racemic crystallites yields racemic mixtures and heterochiral products depending upon the packing arrangement and the reaction pathway (Scheme 1). Consequently, a chiral amplification process of the homochiral oligopeptides can be envisaged (Scheme 1). The enantiomeric excess of the products will depend on the packing arrangement and product distribution within the racemic phase (Scheme 1, and Scheme 2). Within

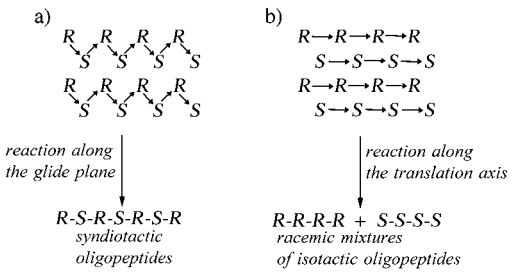

Scheme 2. Schematic representation of the packing arrangement and possible reaction pathways in the 2D racemic crystallites.

these 2D crystallites, the reaction can occur either in a random manner or preferentially, either between heterochiral molecules (Scheme 2a) related by glide symmetry or between homochiral molecules (Scheme 2b) related by translation symmetry.

Different model systems were selected to illustrate our approach: N^{ε}-stearoyl-lysine thioethyl ester (C_{18}-TE-Lys), γ-stearyl-glutamic thioethyl ester (C_{18}-TE-Glu), and γ-stearyl-glutamic acid *N*-carboxyanhydride (C_{18}-Glu-NCA) (Scheme 3). As reference system for a random process, we studied the system of γ-stearyl-glutamic thioacid (C_{18}-thio-Glu) that undergoes an almost random polycondensation, affording a comparison perhaps more realistic than with a theoretical binomial distribution of the products.

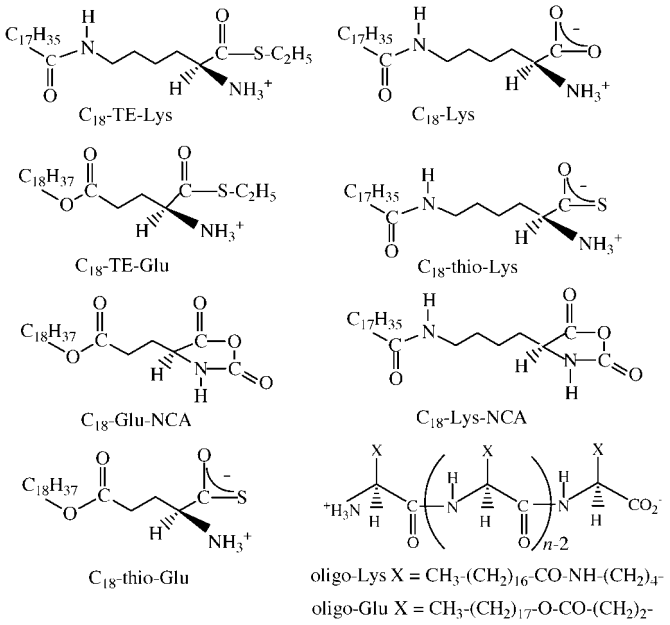

Scheme 3. Model systems selected to illustrate our approach.

The packing arrangements of the 2D crystallites self-assembled at the air–water interface were determined by GIXD using synchrotron radiation. The diastereoisomeric distribution of the oligopeptide products (Scheme 3) starting from various mixtures of monomers enantioselectively labeled with deuterium was determined by matrix-assisted laser-desorption ionization time-of-flight mass spectrometry (MALDI-TOF MS).

Results and Discussion

Packing arrangements of the 2D crystallites on water surface

C_{18}-TE-Lys: Chloroform solutions of enantiomeric (*R*) or (*S*) and racemic (*R*,*S*)-C_{18}-TE-Lys, in the form of their trifluoroacetate salts, were spread on the water surface for a nominal molecular area of 35 Å^2, corresponding to ~70% surface coverage. The *S* enantiomer of racemic C_{18}-TE-Lys incorporated perdeuterated hydrocarbon chains (labeled S_d), leaving the other unlabeled (R_h). The GIXD patterns measured on water from the enantiomeric (*S*) or (*R*) 2D crystallites of C_{18}-

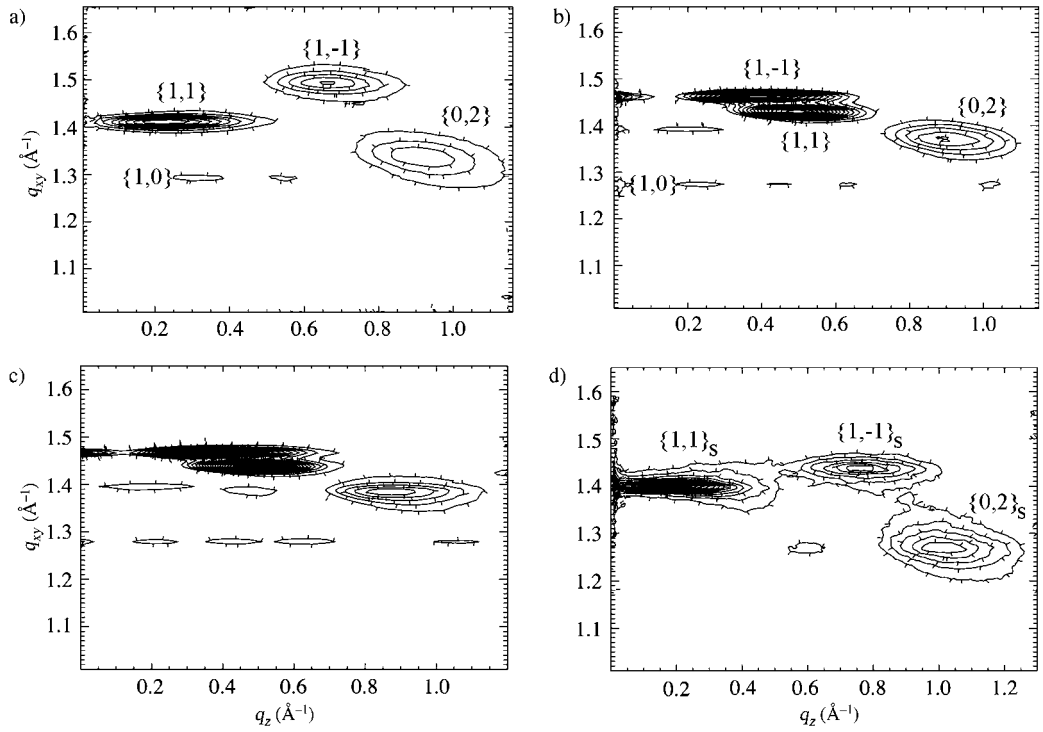

Figure 1. GIXD patterns, represented as two-dimensional contour plots of the scattered intensity as a function of the horizontal q_{xy} and vertical q_z components of the scattering vector, $I(q_{xy},q_z)$, of the self-assembled 2D crystallites of C_{18}-TE-Lys on water at 4 °C prior to (a – c), and after (d) injection of a concentrated aqueous solution of the I_2/KI catalyst beneath the film: a) enantiomerically pure (*S*), (the patterns of (*R*) are identical); b) racemate; c) 2:8 (*R*:*S*) mixture (3:7 (*R*:*S*) is almost identical); d) racemate after a reaction time of 1 – 5 h. In a – c) the {0,1} Bragg rods at $q_{xy} = 0.68$ Å^{-1} are out of range and not shown, for clarity.

TE-Lys are identical but they differ from those of the racemic (*R*,*S*)-C_{18}-TE-Lys (Figure 1a and b).

These patterns also differ from those measured for related compounds such as C_{18}-Lys[34] or C_{18}-thio-Lys[35] showing the influence of the -S-CH_2-CH_3 group. The derived primitive oblique subcell of the enantiomeric phase of C_{18}-TE-Lys, of dimensions $a_S = 4.89$ Å, $b_S = 5.16$ Å, $\gamma_S = 114.3°$, $A_{cell} = 23$ Å^2, is based on the three strong Bragg peaks tentatively assigned (*h*,*k*) Miller indices of $\{0,1\}_S$, $\{1,0\}_S$, and $\{1,-1\}_S$. However, two additional weak reflections at q_{xy} values of 0.685 Å^{-1} (not shown)[36] and 1.291 Å^{-1} indicate that the primitive subcell must be transformed (Scheme 4a) into a centered *pseudo*-rectangular unit cell ($a = a_S$, $b = \boldsymbol{a_S} + 2\boldsymbol{b_S}$) containing two molecules, with $a = 4.89$ Å, $b = 9.43$ Å, $\gamma = 86.1°$. After the transformation, the {*h*,*k*} indices of the strong reflections become {0,2}, {1,1}, and {1, – 1} (Figure 1a) and the two very weak reflections are {0,1} and {1,0}. The molecular chains are tilted 35° from the surface normal along an azimuthal direction of 14° from the *b* axis, as calculated from the q_z positions of the maximum intensity of the Bragg rods. Therefore, the two molecules in the unit cell must have their alkyl chains related by translation since a typical pseudo-herring-bone motif is precluded due to the azimuthal direction of tilt not being along any cell axis. An atomic coordinate molecular model[37] was constructed and the structure was refined by X-ray structure-factor constrained least-squares analysis[38] to fit the five measured Bragg rod intensity profiles (Figure 2a).[39] The resulting 2D packing arrangement viewed normal to the *ab* plane, that is the water surface, is shown in Figure 2b. Intermolecular hydrogen bonds are formed along the *a* axis between the secondary amide groups within the alkyl chains.

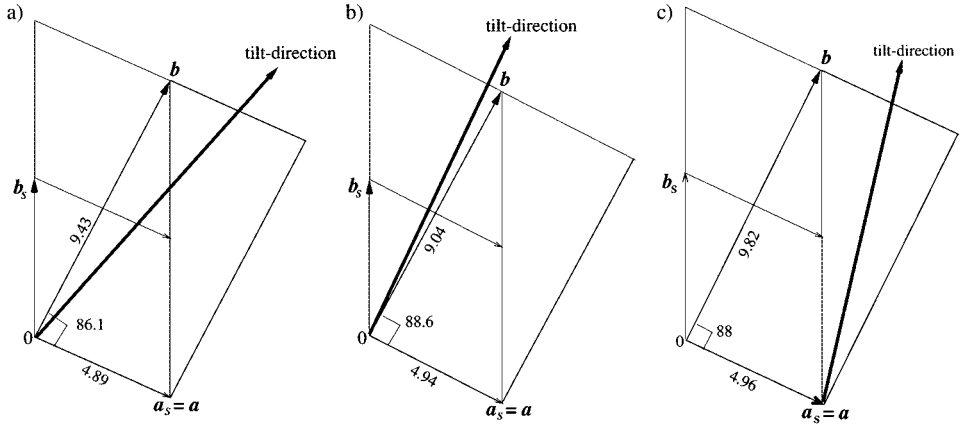

Scheme 4. Drawings of the crystalline unit cells derived from the GIXD data measured from: a) (*R*)- or (*S*)-C_{18}-TE-Lys, b) (*R*,*S*)-C_{18}-TE-Lys, and c) oligopeptide products from enantiomeric and racemic C_{18}-TE-Lys.

The GIXD data from the racemic mixtures of C_{18}-TE-

0947-6539/03/0908-1784 $ 20.00+.50/0 *Chem. Eur. J.* **2003**, *9*, No. 8

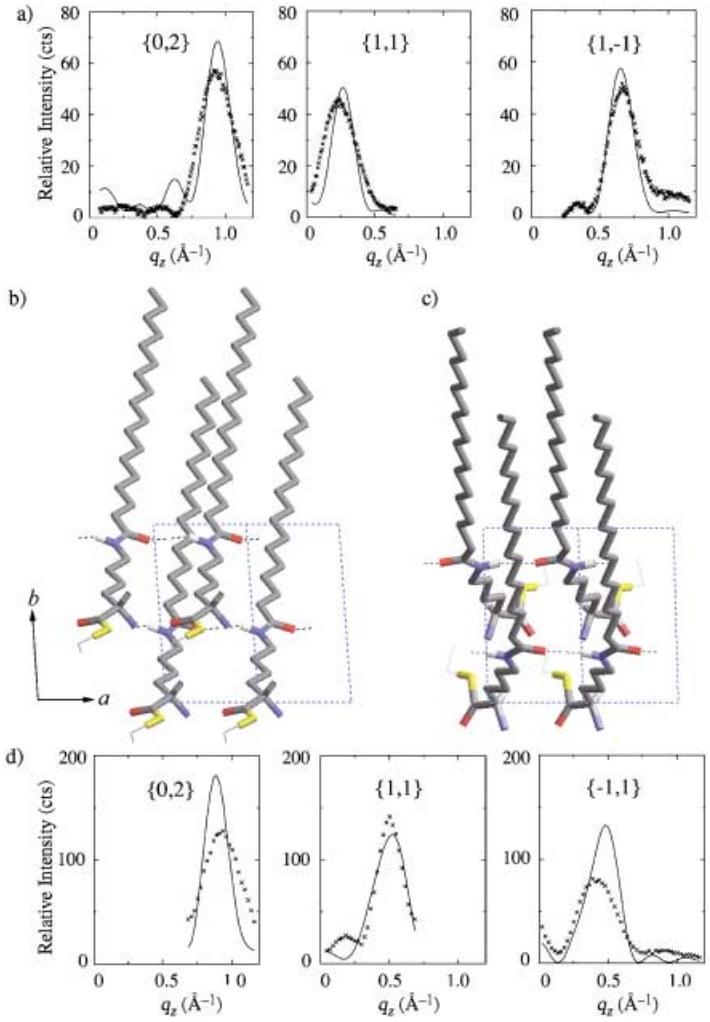

Figure 2. a,d) Measured (x) and calculated (——) Bragg rod intensity profiles $I(q_z)$ and b,c) the corresponding packing arrangements of C_{18}-TE-Lys 2D crystallites viewed perpendicular to the water surface: a,b) Enantiomerically pure and d,c) Racemic. The color code: O red, N blue, S yellow.

Lys yield an almost rectangular unit cell, with $a = 4.94$ Å, $b = 9.04$ Å, $\gamma = 88.6°$, containing two molecules whose alkyl chains are tilted by 33° from the surface normal but in a direction almost parallel to the b axis (Scheme 4b). This result, coupled with the observation that the dimensions of the unit cell projected along the chain axis are $a_p = 4.9$ Å, $b_p = 7.5$ Å, $\gamma_p \approx 90°$, is fingerprint evidence of herring-bone chain packing achieved by pseudo-glide symmetry relating two molecules of opposite handedness. Therefore, the self-assembled 2D crystals are racemic. Their molecular packing arrangement was determined by X-ray structure-factor constrained least-squares refinement (Figure 2c), yielding a reasonably good fit to the measured Bragg rod intensity profiles (Figure 2d).[39]

The self-assembled enantiomeric and racemic C_{18}-TE-Lys 2D crystallites, whose structures were determined by GIXD, were subsequently allowed to react, by injection of catalyst (I_2/KI) into the water subphase, to obtain oligopeptide products. The GIXD patterns measured ¾ to 2 h later showed no presence of the starting monomer phase, but rather the formation of a new crystalline phase belonging to the oligopeptide products (Figure 1d) and which is very similar for both reacted enantiomeric and racemic C_{18}-TE-Lys 2D crystals. These patterns are also very similar to those measured from the crystalline product phase obtained upon polymerization of racemic C_{18}-lysine-N^{α}-carboxyanhydride monomer (C_{18}-Lys NCA) within enantiomorphous 2D crystallites.[35] The three Bragg rods at q_{xy} values of 1.28, 1.40, 1.44 Å^{-1} are consistent with a centered pseudo-rectangular subcell, ($a = 4.96$ Å, $b = 9.82$ Å, $\gamma = 88.0°$), containing two repeat units whose alkyl chains are tilted 38° from the normal to the water surface along an azimuthal direction of 15° from the b axis (Scheme 4c). Such a cell can accommodate oligopeptide repeat units with parallel alkyl chains linked by intramolecular hydrogen bonds along the a axis, as obtained by the reaction occurring preferentially between homochiral molecules related by translation symmetry along the a axis of the monomer phase.[35]

C_{18}-TE-Glu and C_{18}-thio-Glu: To cast light on the influence of an "ester" (-O-CO-) or a "secondary amide" (-HN-CO-) functional groups, contained within the long hydrocarbon chain, on the 2D structures we investigated the packing arrangements of γ-stearyl-glutamic thioethyl ester C_{18}-TE-Glu and γ-stearyl-glutamic thioacid C_{18}-thio-Glu (Scheme 3). The GIXD patterns measured from the self-assembled 2D crystallites of these "glutamate" amphiphiles (Figure 3) are

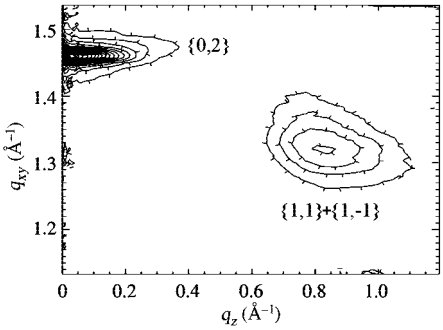

Figure 3. GIXD pattern $I(q_{xy},q_z)$ of the self-assembled 2D crystallites of (*R*,*S*)-C_{18}-TE-Glu (C_{18}-thio-Glu is very similar) on water at 4 °C. Racemates were prepared as mixtures of *S* molecules enantioselectively deuterium-labeled with unlabeled *R* molecules.

significantly different from those measured for the "lysine" counterparts (Figure 2).[35] The GIXD patterns measured from either C_{18}-TE-Glu or C_{18}-thio-Glu whether enantiomerically pure or racemic are almost identical indicating similar arrangements for all the four systems, implying also no contribution (to the scattered intensity) of the -CH_2-CH_3 group connected with the S atom. Despite the limited information of these GIXD patterns it is possible, based on accumulated information,[22] to establish whether molecules in the two racemates pack as a 2D racemic compound or undergo spontaneous separation into enantiomorphous 2D crystallites.

The diffraction patterns exhibit two reflections consistent with a rectangular unit cell containing two molecules, of

dimension $a = 5.8$ Å (5.6 Å for C_{18}-thio-Glu), $b = 8.6$ (8.5 Å for C_{18}-thio-Glu). The long alkyl chains are tilted in the direction of the a axis, as deduced from the q_z position of the maximum intensity of the Bragg rods. In view of the unit cell dimensions, as projected along the molecular chain axis ($\sim$ 4.5 Å $\times$ 8.6 Å), which indicate "shallow" a-glide packing[40] relating molecules of opposite handedness, the 2D crystallites self-assemble from racemate molecules as racemic compounds. The 2D packing arrangement of the racemic 2D crystallites, determined by X-ray structure-factor constrained least-squares refinement of an atomic coordinate molecular model of C_{18}-TE-Glu, together with the measured and calculated Bragg rod intensity profiles, are shown in Figure 4.

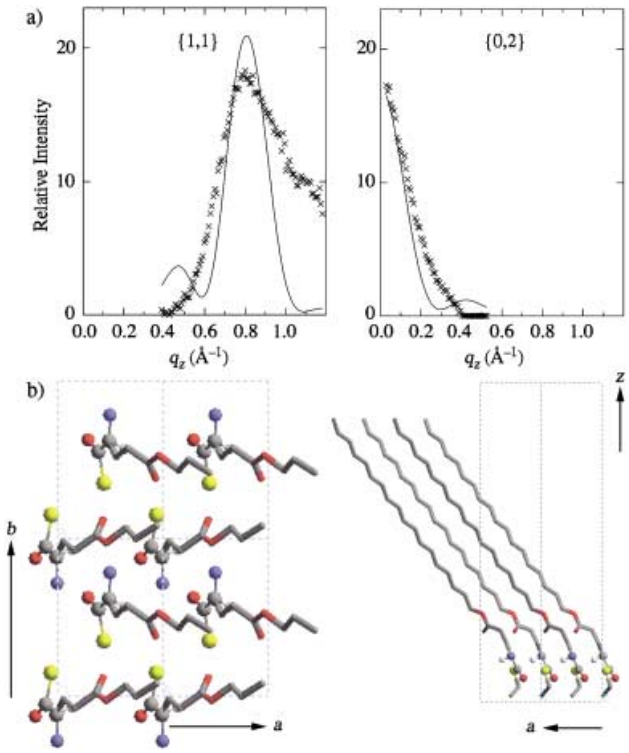

Figure 4. a) Measured (x) and calculated (line) Bragg rod intensity profiles $I(q_z)$; b) refined packing arrangement of (R,S) C_{18}-TE-Glu 2D crystals viewed (left) perpendicular to the water surface and (right) parallel to the water surface along the b axis. The color code: O red, N blue, S yellow.

The molecules within the 2D crystallites of racemic C_{18}-TE-Glu are enantiomerically ordered, presumably due to the bulky -S-CH_2-CH_3 groups, as deduced from the MALDI-TOF MS results (see below). For racemic C_{18}-thio-Glu, which embodies a zwitterionic (-HC*-(NH_3^+)-COS^-) head group, enantiomeric and conformational disorder is present, as deduced again from the MALDI-TOF MS results (see below).

In the (R) or (S) crystallites, self-assembled from enantiomeric C_{18}-TE-Glu or C_{18}-thio-Glu, the pure glide symmetry is forbidden, yet the structure may resemble that of the racemate. This mimicry may be achieved by a pseudo-glide arrangement of the molecular chains, but the head groups are related by pseudo-translation.

The GIXD patterns measured from the 2D crystals of (R,S) C_{18}-TE-Glu and C_{18}-thio-Glu did not change after injection of the catalyst into the water subphase.[41] MALDI-TOF MS analysis of samples taken from the air–water interface before catalyst addition showed the presence only of the starting monomers, whereas after catalyst addition the oligopeptide products were found.

Enantiomeric composition of the products from MALDI-TOF MS: This analysis was employed to determine the number of the R and S units within each oligopeptide molecule obtained in the polycondensation reaction. For this purpose, one of the reactant enantiomers was labelled with a perdeuterated alkyl chain. As a result of the enantioselective labeling of only the S enantiomer with deuterium we obtain a mass difference per peptide repeat unit of $\Delta m/z$ 35 mass units for C_{18}-TE-Lys and 37 for C_{18}-thio-Glu and C_{18}-TE-Glu.[20, 42]

The MALDI-TOF MS analysis was performed on samples collected from the interface two to four hours after aqueous solutions of catalysts (I_2/KI, or $AgNO_3$) were injected into the water subphase beneath the 2D crystallites.[43, 44] According to the MALDI-TOF MS analysis (see Experimental Section), the products prepared by polycondensation of (R,S)-C_{18}-TE-Lys contain a mixture of di- to hexapeptide products of various composition. The total ion abundance of the different oligopeptides, normalized to that of the dipeptide product obtained from C_{18}-TE-Lys exhibits an exponential decrease with increasing length of the oligopeptides (Figure 5). Similar

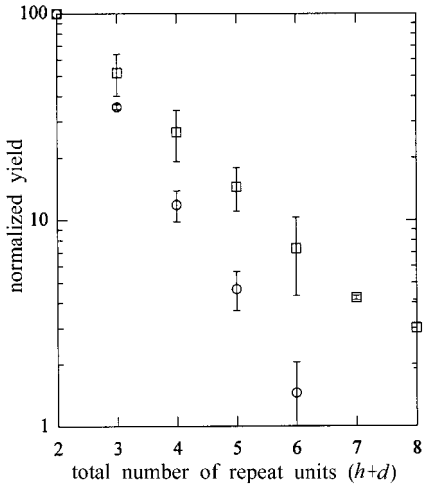

Figure 5. The normalized yield, defined as the relative intensity of the various oligopeptides normalized to that of the dipeptide, shown for each oligopeptide length with a total number of repeat units $n = h + d = 2-8$: (○) C_{18}-TE-Lys (□) C_{18}-thio-Glu. The error bars include the uncertainties obtained by studying different mass spectra of different prepared samples, different deposits of the same sample and different spots on a same sample.

behavior was observed for (R,S)-C_{18}-thio-Glu (up to octa-peptides), (R,S)-C_{18}-TE-Glu (up to penta-peptides) and C_{18}-Glu-NCA (up to dodeca-peptides). In the total m/z range, the ionization yield and detection efficiency can depend on the peptide length. Thus the observed exponential decay gives only a trend. However, the *comparison* (Figure 5) between (R,S)-C_{18}-TE-Lys and (R,S)-C_{18}-thio-Glu is more relevant since both compounds are observed in a similar mass range and thus with very similar detection efficiency.

0947-6539/03/0908-1786 $ 20.00+.50/0 *Chem. Eur. J.* **2003**, *9*, No. 8

Although we cannot differentiate between diastereomeric oligopeptides containing the same number of *R* and *S* units, the method does allow us to differentiate enantiomers of both homochiral and heterochiral oligopeptides. For oligopeptides of the same length, the observed ion intensity in the MALDI-TOF spectra and the amount of molecules are reliably proportional. The chemical properties of such oligopetides are similar and their ionization efficiencies are expected to be identical. Indeed, for such oligopeptides, with similar chemical properties and comparable masses and velocities in the TOF mass spectrometer, ionisation yield and detection efficiency are expected to be identical. Thus we can reliably express the composition of the oligopeptides in terms of a relative abundance *ra* (*h*,*d*), (where *h* is the number of *R*(unlabeled) units and *d* the number of *S*(deuterated) units) for molecules of each length. This relative abundance was obtained by division of the intensity of all the ions corresponding to each molecule to the intensity of the ions from all the molecules of the same length (see Experimental Section).

The relative abundance of the different diastereoisomers for each oligopeptide length obtained from the polycondensation reaction of racemic C_{18}-TE-Lys with I_2/KI catalyst have a distribution (Figure 6a) that reveals a clear trend towards enhanced formation of homochiral R_h and S_d peptides vis-à-vis their heterochiral counterparts. When the reaction was catalyzed by addition of Ag^+ ions injected into the water subphase, a similar distribution of the oligopeptides, especially for the tetra-, penta-, and hexapeptides, was obtained (Figure 6b). The relative abundance of the di- and tripeptides

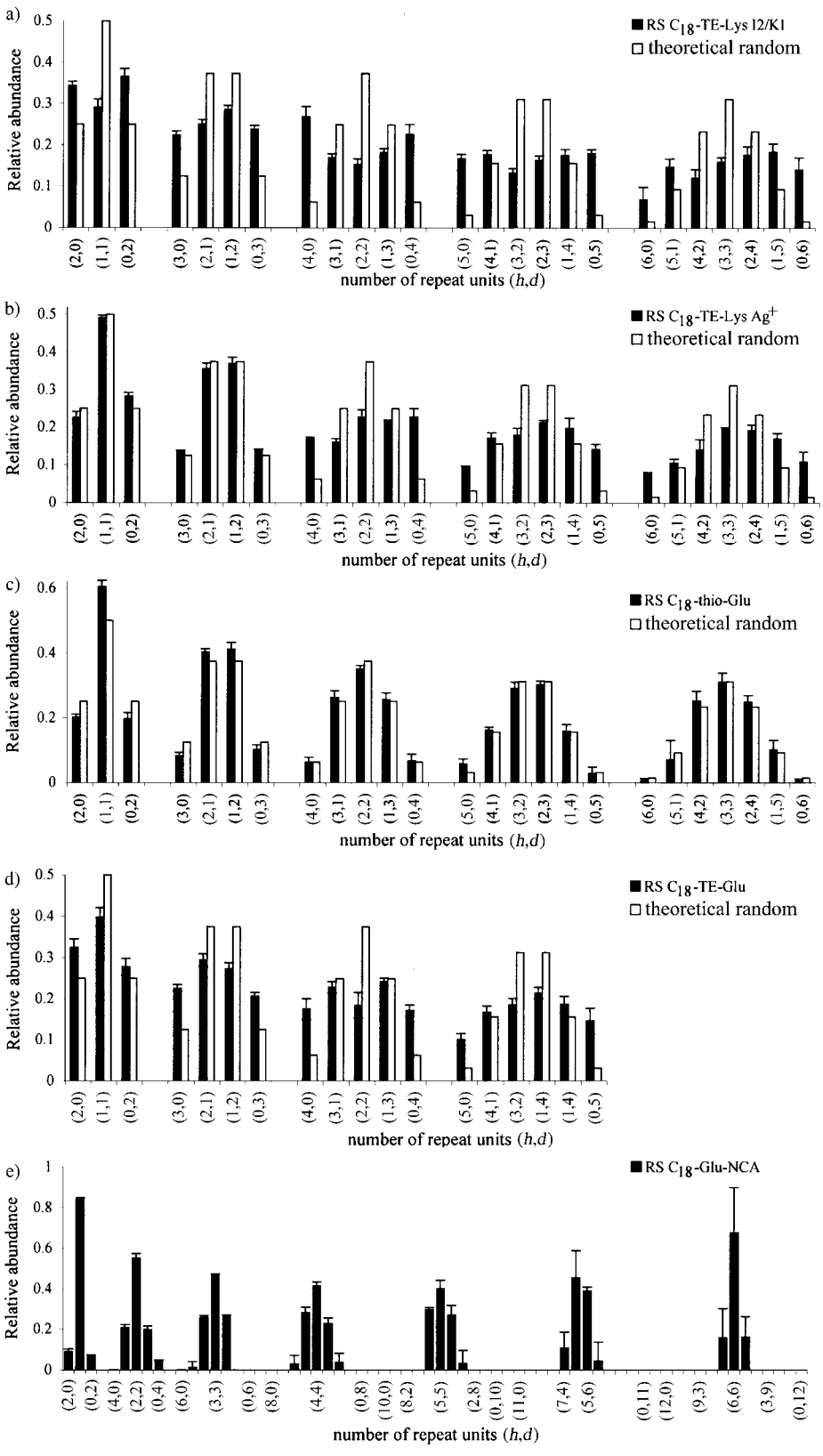

Figure 6. MALDI-TOF MS analysis of the oligopeptides obtained at the air–water interface from racemic mixtures of monomers, 2 h after injection of concentrated aqueous solutions of various catalysts: a, b) C_{18}-TE-Lys, I_2/KI and $AgNO_3$ catalysts, respectively; c, d) C_{18}-thio-Glu and C_{18}-TE-Glu, I_2/KI catalyst; e) C_{18}-Glu-NCA, $Ni(CH_3CO_2)_2$ catalyst. The histograms show the relative abundance of each experimentally obtained oligopeptide, (solid bars), compared to those calculated for a binomial distribution in a theoretically random process (empty bars). For clarity, histogram in e) shows the distribution of only some of the oligopeptides, namely those with $h+d=2$, 4, 6, 8, 10, 11, 12.

  0947-6539/03/0908-1787 $ 20.00+.50/0

with homochiral sequence is smaller compared to that obtained using I_2/KI catalyst, reflecting a different reaction mechanism.[45] For comparison, Figure 6c shows the distribution of oligopeptides obtained from the polycondensation of racemic C_{18}-thio-Glu that yielded essentially a random distribution of the diastereoisomeric oligopeptides (Figure 6a, b, c empty bars). Therefore C_{18}-thio-Glu provides an experimental reference system, more realistic than the theoretical values for a binomial distribution in a random process. This result implies that the racemic C_{18}-thio-Glu crystallizes with enantiomeric disorder of the head groups, as proposed above. A comparison between Figure 6a, b, and c shows a distinct bias for the C_{18}-TE-Lys system to form homochiral diastereoisomers, labeled (*h*,0) and (0,*d*), at the extremities of each distribution for di- to hexapeptides. The enhanced concentration of the homochiral C_{18}-TE-Lys oligopeptides, (Figure 6a,b), is in agreement with the packing arrangement of this racemic monomer (Figure 2c). The amino group of one molecule is appropriately oriented and in close proximity to a carbonyl group of a nearest neighbor homochiral molecule (~5.0 Å) to react and form a peptide bond (Figure 7a, left). In contradistinction, the amine and carbonyl groups of two heterochiral molecules related by glide symmetry are less appropriately aligned for a nucleophilic attack (Figure 7a, right).

The distribution of the different diastereoisomers for each oligopeptide length obtained in the polycondensation of the racemic C_{18}-TE-Glu (Figure 6d) reveals a trend similar to that of the C_{18}-TE-Lys system towards enhanced formation of homochiral R_h and S_d peptides vis-à-vis their heterochiral counterparts, especially for tri-, tetra-, and pentapeptides. Once again, molecules related by translation along the *a* axis within the racemic monomer 2D crystallites undergo preferred condensation. However, this system was found to be less reactive than C_{18}-TE-Lys yielding a mixture of di- to pentapeptides and the relative abundance of the homochiral R_h and S_d peptides is smaller compared to that of C_{18}-TE-Lys. According to the packing arrangement of racemic C_{18}-TE-Glu, the distance between the N(amino) and C(carbonyl) atoms is smaller for molecules related by glide symmetry than by translation symmetry, however the reaction occurs preferentially between homochiral molecules related by translation, presumably because the SN2 reaction pathway appears to depend on the orientation of these groups in the 2D crystallites (Figure 7b, right, left).

Chiral amplification of the oligopeptides: We will now describe the structure and the polycondensation behavior of non-racemic C_{18}-TE-Lys monomers and non-racemic C_{18}-TE-Glu monomers at the air–water interface. The MALDI-TOF MS results clearly show a distinct enhancement of the homochiral fraction of the S_d oligopeptides (0,*d*) relative to that of the heterochiral molecules (*h*,*d*) obtained, especially for penta- to hexa- (hepta-)peptides, upon polycondensation of 3:7 and 4:6 (*R*:*S*) mixtures of C_{18}-TE-Lys monomers (Figure 8a,c). The diastereoisomeric composition of the oligopeptide products is compared not only with the theoretical values for a random process (Figure 8a, c empty columns) but, once again, with C_{18}-thio-Glu (Figure 8b, d), our experimental reference system for random polymerization. Enhanced formation of the homochiral products was obtained also for the 3:7 and 4:6 (*R*:*S*) mixtures of C_{18}-TE-Glu monomers (Figure 9).

Analysis of the experimental results shows that when starting with 3:7 and 4:6 (*R*:*S*) mixtures of C_{18}-TE-Lys, the relative abundance of the homochiral (*S*)-hexapeptides normalized to the corresponding experimental values obtained for the C_{18}-thio-Glu have enhancement factors of 2.2 and 2.0, respectively. For the C_{18}-TE-Glu system, the normalized enhancement factor is 2.0 for both (*S*)-hexapeptides and (*S*)-pentapeptides, obtained from 3:7 and 4:6 (*R*:*S*) mixtures, respectively, of the monomer. These enhancement factors imply a phase separation of the starting non-racemic mixture of monomers into racemic and enantiomorphous 2D crystallites and the polycondensation reaction taking place within such separate domains.

The GIXD patterns measured from the enantiomorphous and racemic 2D crystallites of C_{18}-TE-Glu are very similar, therefore in the diffraction patterns we could not detect a phase separation of the non-racemic mixtures. By comparison, the GIXD patterns measured from the enantiomorphous and racemic 2D crystallites of C_{18}-TE-Lys are significantly different. Monolayer samples of racemic and non-racemic mixtures of C_{18}-TE-Lys prepared from the same number of molecules were measured by GIXD. However, the patterns measured from 3:7 (*R*:*S*) mixtures of C_{18}-TE-Lys (Figure 1c) were very similar to those measured from the racemate (Figure 1b) in terms of the positions in q_{xy} and q_z components of the scattering vector corresponding to the Bragg rods as well as their intensities. These results indicate that the crystallinity in the racemic and non-racemic samples is

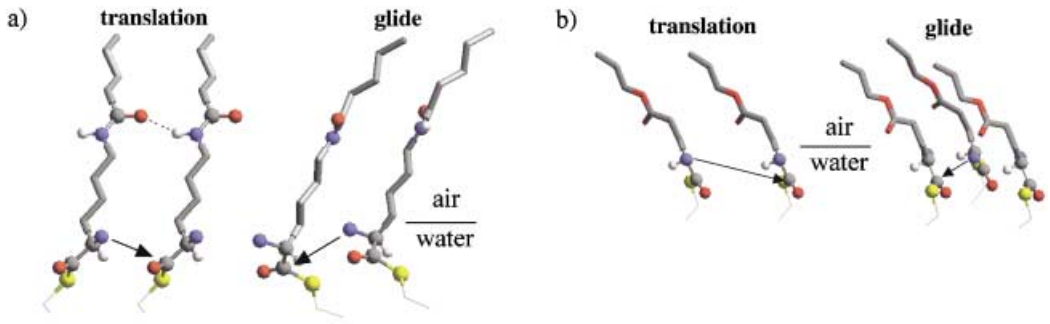

Figure 7. Pairs of a) C_{18}-TE-Lys and b) C_{18}-TE-Glu molecules related by translation and by glide symmetry in their racemic 2D packing arrangements shown respectively in Figure 2c and Figure 4b, viewed parallel to the water surface. For clarity, only part of the hydrocarbon chains is shown.

0947-6539/03/0908-1788 $ 20.00+.50/0 *Chem. Eur. J.* **2003**, *9*, No. 8

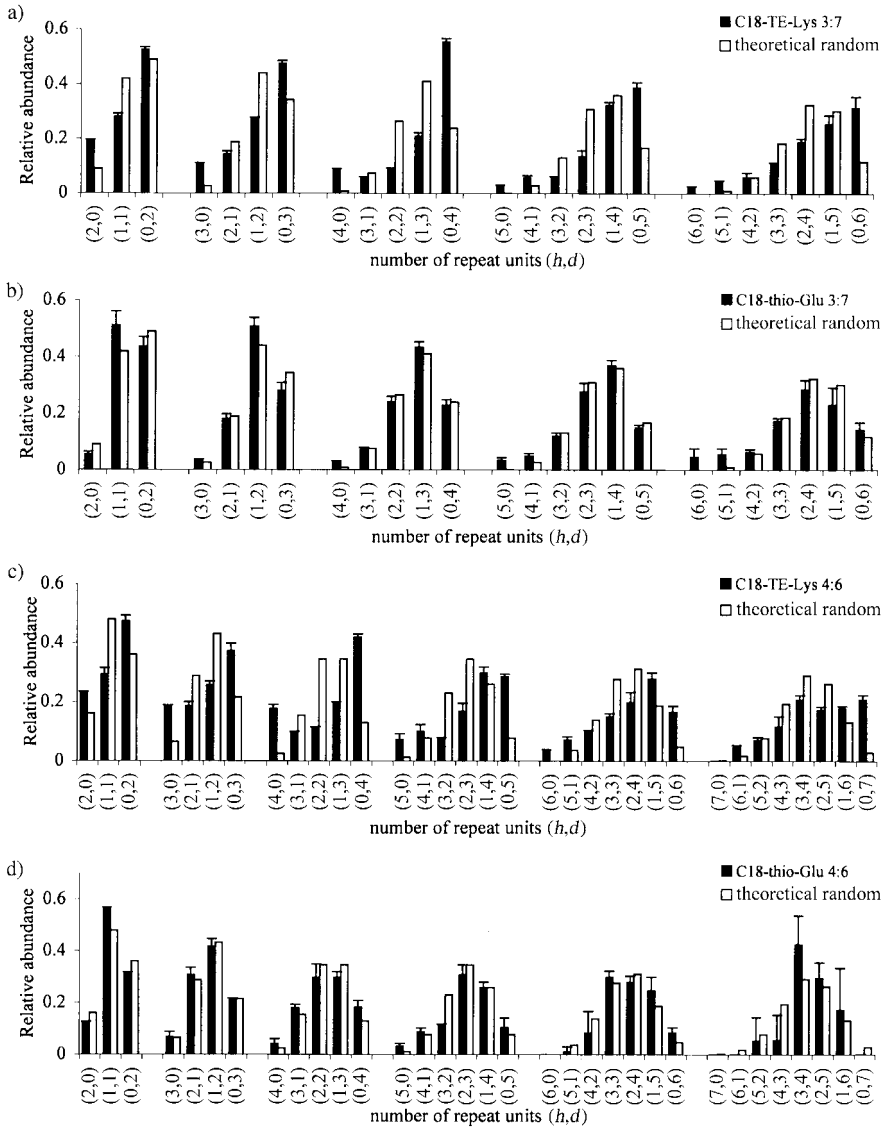

Figure 8. MALDI-TOF MS analysis. Relative abundance of the oligopeptides obtained, at the air–water interface, from non-racemic mixtures of monomers (solid bars) compared to those calculated for a theoretical random process (empty bars): a, b) 3:7 (*R*:*S*) and c, d) 4:6 (*R*:*S*) C_{18}-TE-Lys and C_{18}-thio-Glu non-racemic mixtures of monomers, respectively.

similar. Two possible packing modes can be envisaged for the non-racemic mixtures of C_{18}-TE-Lys, either the formation of a random solid solution or the excess of *S*-molecules crystallizes in a "phase" similar to the racemate. In view of the MALDI-TOF MS results we eliminate the formation of a solid solution. A way to rationalize the packing arrangement of the 3:7 (*R*:*S*) mixtures of C_{18}-TE-Lys is in terms of a line epitaxial crystallization of the enantiomorphous (*S*)-"phase" alongside the racemic "phase" with the interfacial "line" perpendicular to the "*a*" axis (4.9 Å).[46] This "epitaxy" may have been promoted by the intermolecular hydrogen bonds along the *a* axis between the secondary amide groups within the alkyl chains and which induced a change in the tilt direction of the alkyl chains of the enantiomorphous "phase" as to resemble the racemic "phase". This model is reinforced by the GIXD pattern of the 2:8 (*R*:*S*) mixture of C_{18}-TE-Lys (Figure 1c), which is also very similar to that of the racemate (Figure 1b).[47]

The relative abundance of the homochiral oligopeptides determined by MALDI-TOF MS was used to calculate the enantiomeric excess (*ee*) for oligopeptide molecules of each length obtained from the non-racemic mixtures of the three monomer systems (Table 1). As seen from Table 1, the *ee* values of the homochiral oligopeptides obtained from C_{18}-TE-Lys and C_{18}-TE-Glu increase with the length and are higher than the *ee* of the corresponding mixture of monomers. The *ee* values calculated for the C_{18}-thio-Glu system, that undergoes an almost random polycondensation are apparently high; however the relative abundance of the longer homochiral oligopeptides is very low (Figure 8b, d) as in any random process.

Due to complexity of the factors that affect the reactivity within two-phase systems, it is difficult to explain these values of *ee*. on a quantitative basis. Qualitatively, however, several aspects depending on the structure and reactivity within the racemic 2D crystallites clearly influence the *ee*. Oligopeptide products of various

Table 1. Comparison between the enantiomeric excess (*ee*)[a] obtained upon polycondensation of 3:7 and 4:6 (*R*:*S*) mixtures of C_{18}-TE-Lys monomers, C_{18}-TE-Glu monomers, and C_{18}-thio-Glu monomers.

Starting monomer	3:7 (*R*:*S*) *ee* = 40			4:6 (*R*:*S*) *ee* = 20		
peptide	C_{18}-TE-Lys	C_{18}-TE-Glu	C_{18}-thio-Glu	C_{18}-TE-Lys	C_{18}-TE-Glu	C_{18}-thio-Glu
di-	46	48	78	34	27	42
tri-	63	71	80	34	39	54
tetra-	73	82	78	41	46	67
penta-	85	91	63	60	59	77
hexa-	86	> 99.8	51	62	–	98
hepta-	–	–	0	> 99.8	–	0

[a] The values of the enantiomeric excess calculated according to $ee = 100([S]-[R])/([S]+[R])$, where [*S*] and [*R*] represent the experimental relative abundance for the homochiral oligopeptides of each length.

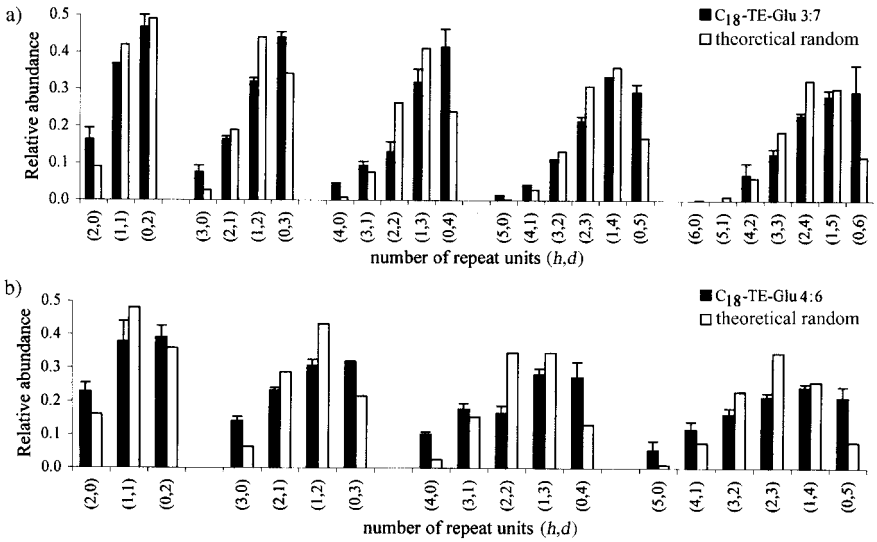

Figure 9. MALDI-TOF MS analysis; Relative abundance of the oligopeptides obtained, at the air–water interface, from non-racemic mixtures of monomers (solid bars) as compared to those calculated for a theoretical random process (empty bars): 3:7 (a)

lengths may be formed within each of the two phases. For example, only (*S*)-heptapeptides were formed from the 4:6 (*R*:*S*) mixtures of C_{18}-TE-Lys (Figure 8c) and only (*S*)-hexapeptides from the 3:7 (*R*:*S*) mixtures of C_{18}-TE-Glu (Figure 9a), products that were not obtained from the corresponding racemates.

The polycondensation reaction occurring between homochiral molecules, related by translation symmetry (Scheme 2b) within the racemic monomer phases of the C_{18}-TE-Lys and C_{18}-TE-Glu systems, resulted in the formation of the homochiral oligopeptides from the minor monomer leading to a reduction of the *ee*. To circumvent this drawback, a system was selected where the polymerization reaction within the racemic monomer phase occurs between heterochiral molecules related by glide symmetry (Scheme 2a), to form syndiotactic oligopeptides. Consequently, oligopeptides that are homochiral and of a single handedness will be formed only within the enantiomorphous 2D crystallites of the two-phase system of the monomers, as demonstrated for the system of C_{18}-Glu-NCA.

The GIXD pattern, (Figure 10a, top), measured from the enantiomeric C_{18}-Glu-NCA spread on water for a nominal molecular area of 35 Å^2, yields a pseudo-rectangular unit cell of dimension $a = 5.52$ Å, $b = 8.62$ Å, $\gamma = 92.5^\circ$. From the q_z positions of the maximum intensity of the three Bragg rods we derive that the molecular chains are tilted by 34.8° from the surface normal in a direction 15° off the *a* axis. The refined 2D molecular arrangement and the corresponding Bragg rod intensity profiles are shown in Figure 10a (middle, bottom). Injection of catalyst (nickel acetate) into the water subphase induces a reaction that could be observed by GIXD yielding a pattern similar to that shown in Figure 10b (top). A minor, yet significant, change occurs in the unit cell that becomes rectangular ($a = 5.54$ Å, $b = 8.58$ Å, $\gamma = 90^\circ$), in keeping with chains of the polymerized film tilted by 34° from the surface normal in a direction parallel to the *a* axis.

The GIXD patterns of racemic C_{18}-Glu-NCA on pure water (Figure 10b, top), and on aqueous solution containing catalyst are similar, namely, no change in the diffraction pattern was observed during the reaction. The refined 2D packing arrangement of the C_{18}-Glu-NCA monomer molecules self-assembled into racemic 2D crystallites and the corresponding Bragg rod intensity profiles are shown in Figure 10b (middle, bottom).

Note that the diffraction pattern of racemic C_{18}-Glu-NCA is very similar to those measured from enantiomeric and racemic C_{18}-TE-Glu and C_{18}-thio-Glu (Figure 3), however the pathway of the polymerization reaction is very different. As described above, C_{18}-TE-Glu self-assembled into racemic ordered 2D crystallites and the reaction occurred preferentially between homochiral molecules along the *a* axis, due to appropriate head group orientation and in spite of the fact that the relevant intermolecular distance is smaller for molecules related by glide symmetry. By contrast, according to the packing arrangement of the racemic 2D crystallites of C_{18}-Glu-NCA, a lattice-controlled polymerization can occur primarily between heterochiral molecules related by glide symmetry (Scheme 2a). Such a pathway occurs, presumably, due to the appropriate "herringbone" orientation of the rigid *N*-carboxyanhydride moieties. Indeed, the MALDI-TOF MS results are in agreement with the proposed reaction pathway. The distribution of various oligopeptides (Figure 6e) obtained upon polymerization of the racemic monomer shows the formation of heterochiral oligopeptides in concentrations beyond the theoretical random distribution and significantly different from those of C_{18}-TE-Lys, C_{18}-TE-Glu, and C_{18}-thio-Glu (Figure 6a–d).

Consequently, a most efficient chiral amplification process was anticipated for the non-racemic mixtures of C_{18}-Glu-NCA that may undergo a separation into racemic and enantiomeric phases. The former (i.e. racemic) primarily yields heterochiral oligopeptides, whereas the latter (i.e. enantiomeric) yields oligopeptides that are homochiral and of a single handedness. The MALDI-TOF MS results clearly demonstrate the formation of short oligopeptides rich in heterochiral diastereoisomers, whereas the longer oligopeptides obtained from 3:7 and 4:6 (*S*:*R*) mixtures of monomers are rich in homochiral sequences of single handedness (Figure 11a, b). Oligopeptides nine or ten units long obtained from the 3:7 (*S*:*R*) mixtures of monomers comprise only compositions 1*S*:8*R* and 0*S*:9*R* or 1*S*:9*R* and 0*S*:10*R* , labeled (1,8), (0,9) and (1,9), (0,10) respectively (Figure 11a). Similarly the 4:6 (*S*:*R*) mixtures yielded octa- and nonapeptides of only 1*S*:7*R* and 0*S*:8*R* or 1*S*:8*R* and 0*S*:9*R* compositions, labeled (1,7), (0,8) and (1,8), (0,9), respectively (Figure 11b).

0947-6539/03/0908-1790 $ 20.00+.50/0 *Chem. Eur. J.* **2003**, *9*, No. 8

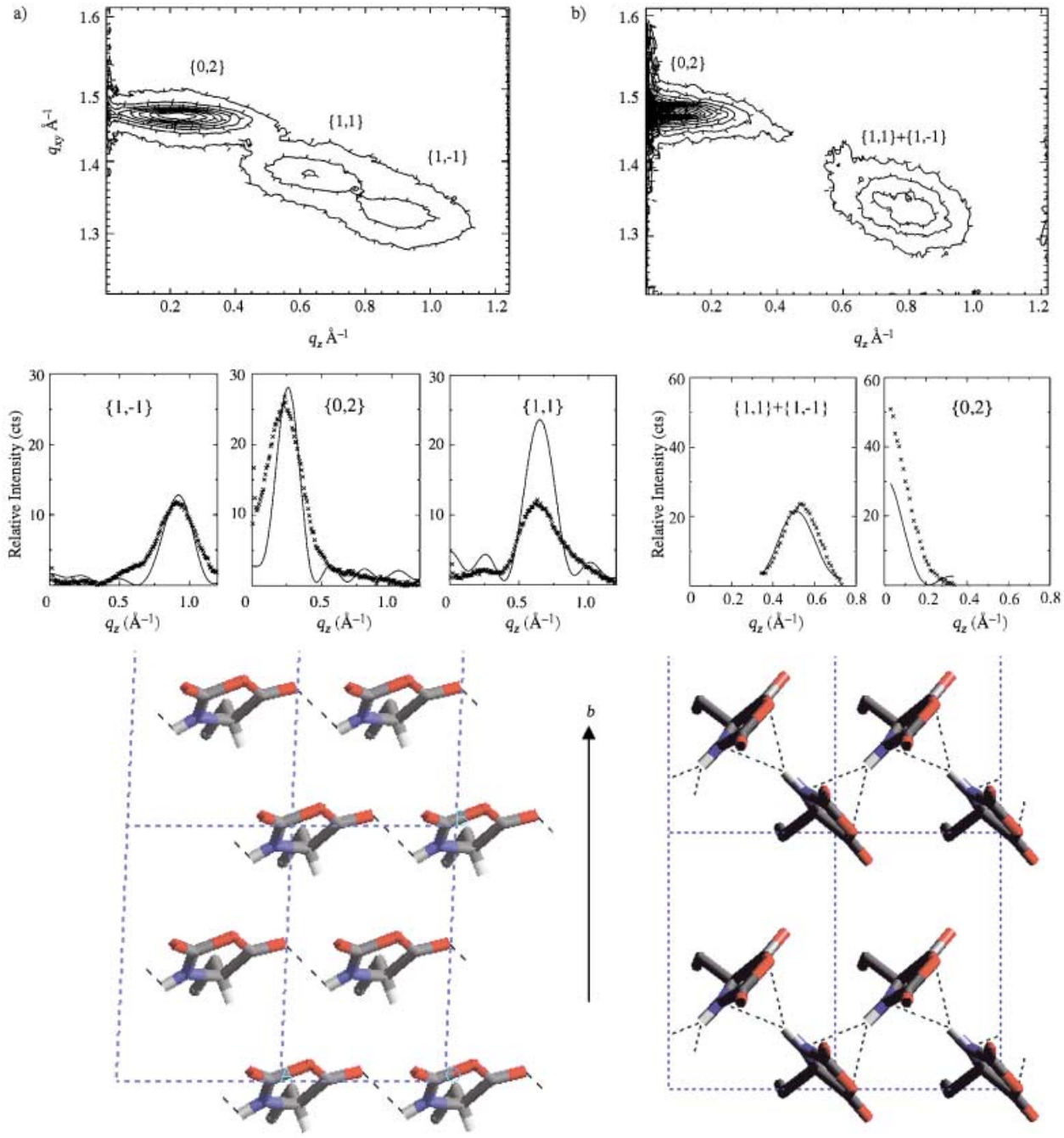

Figure 10. GIXD patterns $I(q_{xy},q_z)$, measured (x) and calculated (——) Bragg rod intensity profiles and the refined packing arrangements, viewed perpendicular to the water surface, of the C_{18}-Glu-NCA 2D crystallites: a) enantiomerically pure and b) racemic. For clarity, only the N^{α}-carboxyanhydride ring is shown.

Conclusion

The feasibility of obtaining homochiral oligopeptides with high relative abundance starting from racemic monomers that pack in the form of 2D racemic compounds has been demonstrated for the C_{18}-TE-Lys and C_{18}-TE-Glu systems. The analysis of the GIXD data yielded the precise packing of the hydrocarbon chains and a determination of the head group packing to near atomic resolution where constraints had been imposed on the intra- and intermolecular distances. The correlation between the 2D packing arrangements of the monomers and the composition of the various diastereoisomeric products is not straightforward. The enhanced formation of the homochiral oligopeptides from the C_{18}-TE-Lys monomer could be rationalized by taking into consideration the favorable orientations of the amine and carbonyl groups prior to the formation of the peptide bonds. The preferred formation of heterochiral oligopeptides could also be correlated with the 2D packing arrangement of the C_{18}-Glu-NCA monomer. These results provide *prima-facie* evidence that the polymerization reaction is lattice-controlled. There is no simple correlation, however, between the 2D packing ar-

  0947-6539/03/0908-1791 $ 20.00+.50/0

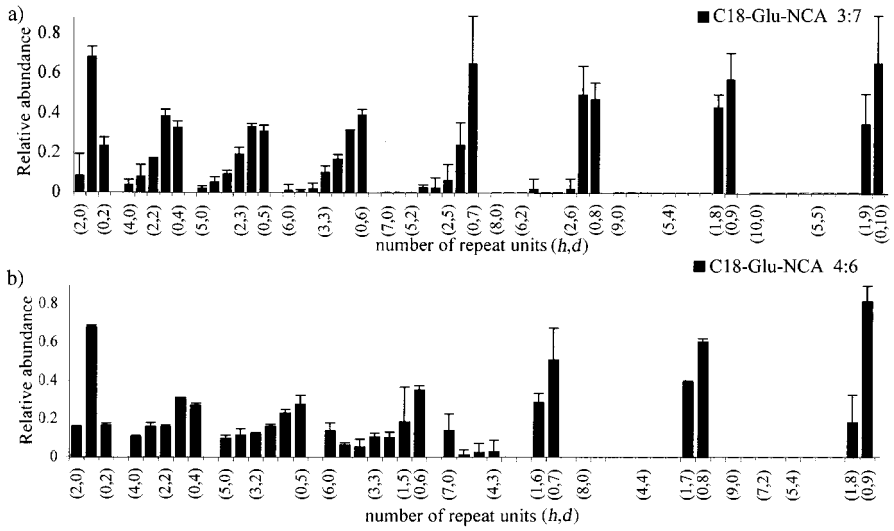

Figure 11. MALDI-TOF MS analysis; Relative abundance of the oligopeptides obtained, at the air–water interface, from non-racemic mixtures:

rangement of the C_{18}-TE-Glu monomer and the diatereoisomeric composition of the products. We can only rationalize the preferred formation of oligopeptides of homochiral sequence by assuming a structural change that might have occurred in the polar head groups during the polymerization reaction, without causing a measurable change in the GIXD patterns.

Lattice-controlled reactions within such self-assemblies also provide ways to generate homochiral oligopeptides of a single handedness from non-racemic mixtures of monomers with a low enantiomeric imbalance. The amplification of chirality requires that the non-racemic monomers self-assemble such that the racemic component forms racemic 2D crystallites comprising both enantiomers, whereas the fraction of the enantiomer in excess separates into enantiomorphous 2D crystallites. Such phase separation follows from the distribution of the diastereisomeric oligopeptides determined by MALDI-TOF MS analysis in all the three systems.

The *ee* of the homochiral oligopeptides is determined by the packing arrangement and the reaction pathway within the racemic 2D crystalline phase.[48] The highest *ee* is obtained in systems where the reactivity within the racemic phase occurs solely between heterochiral molecules to yield heterochiral oligopeptides whereas the fraction of the enantiomer in excess yields homochiral oligopeptides of the corresponding handedness.

The kinetics of polymerization within the racemic and enantiomorphous crystalline phases should be different. Consequently, the distribution of the oligopeptides of different length obtained from the two phases should not be identical. This difference implies that in systems where longer oligopeptides are formed in the enantiomorphous phase, they should be of a single handedness, as for example, in the C_{18}-Glu-NCA systems.

The success of such amplification processes depends on the degree of phase separation of the non-racemic mixtures of monomers. From the systems described here, only the C_{18}-TE-Lys was amenable to study also by GIXD since for the other systems the diffraction patterns of the enantiomerically pure and racemic monomers were very similar. The GIXD patterns measured from non-racemic mixture of C_{18}-TE-Lys are almost identical to those of the racemate. However, the MALDI-TOF MS analysis of the product distribution clearly demonstrated the phase separation. On this basis, the GIXD results (including Bragg peak intensities) could be rationalized in terms of a change in the packing arrangement of the enantiomorphous phase as induced by the racemic phase.[47] Consequently, several analytical methods must be used for the complete characterization of the systems.

Finally, lattice-controlled polymerization within 2D crystalline self-assemblies are associated with the appearance of nonlinear effects[49] that may lead, in appropriate systems, to efficient chiral amplification in the formation of biomolecules and therefore should be of relevance to prebiotic chemistry. Optimization of such processes, by providing a deeper insight into the detailed structures of the 2D crystallites as well as by clarifying the precise reaction pathway, is required. Investigations along these lines are underway.

Experimental Section

Materials: *R*- and *S*-N^{ε}-stearoyl-lysine-thioethyl ester (C_{18}-TE-Lys) and *R*- and *S*-γ-stearyl-glutamic-thioethyl ester (C_{18}-TE-Glu) were synthesized by the reaction of the corresponding N^{ε}-Stearoyl-Lys(Boc) and γ-stearyl-Glu(Boc) with thioethanol followed by removal of the Boc protecting group with trifluoacetic acid. N^{ε}-Stearoyl-Lys(Boc) was synthesized by the reaction between with *N*-hydroxysuccinimide of stearic acid and Boc-Lys-OH (BACHEM AG), according to standard procedures. For the normal series of compounds, we used stearic acid (Aldrich) and for deuterated compounds we used perdeuterated stearic acid (D35 98% Cambridge Isotope Laboratories). γ-Stearyl-Glu(Boc) was synthesized from the reaction of Boc-Glu-OFm (BACHEM AG) with stearyl alcohol (Aldrich) for the normal series of compounds and per-deuterated stearyl alcohol (D37 98% EuroIsotope) for deuterated compounds.

N^{ε}-carboxyanhydrides of *R*- and *S*-γ-stearyl-glutamic acid (C_{18}-Glu-NCA) were synthesized from the corresponding long-chain amino acid γ-stearyl-glutamic acid (C_{18}-Glu), according to a reported procedure.[50] In the synthesis of C_{18}-Glu we used either stearyl alcohol or per-deuterated stearyl alcohol.[51] *R*- and *S*-γ-stearyl-glutamic thio-acid(C_{18}-thio-Glu) were obtained from the corresponding C_{18}-Glu-NCA with H_2S in the presence of 2,6-lutidine at $-10\,^{\circ}C$.[52]

Characterization of compounds

***R*-, *S*- C_{18}-TE-Lys ($C_{17}H_{35}$ chain)**: ^{1}H NMR (400 MHz): $\delta = 0.9$ (t, 3H), 1.27 (br m, 31H), 1.45–1.8 (br m, 8H), 2.16 (t, 2H), 2.9 (q, 2H), 3.28 (q, 2H), 3.51 (t, 1H) 5.5 ppm (s, 1H); FTIR (KBr pellet): $\tilde{\nu} =$ 3327, 2928, 2859, 1702, 1642, 1549, 1463, 1208, 1141 cm^{-1}; ESI-MS: *m/z*: 457.8 [$M^+ + H$].

***R*-, *S*-C_{18}-TE-Lys ($C_{17}D_{35}$ chain)**: ^{1}H NMR (400 MHz): $\delta = 1.27$ (t, 3H), 1.45 (m, 2H), 1.5–1.8 (m, 6H), 2.88 (q, 2H), 3.28 (q, 2H), 3.5 (t, 1H) 5.6 ppm (s,

0947-6539/03/0908-1792 $ 20.00+.50/0 *Chem. Eur. J.* **2003**, *9*, No. 8

1H); FTIR (KBr pellet): $\tilde{\nu}$ = 2919, 2853, 1702, 1642, 1549 cm^{-1}; ESI-MS *m/z*: 492.9 [$M^+ + H$].

C_{18}-thio-Glu ($C_{18}H_{37}$ chain): ^{1}H NMR (400 MHz): δ = 0.9 (t, 3H), 1.3 (br m, 30H), 1.77 (m, 2H), 2.5–2.6 (m, 2H), 2.90 (t, 2H), 4.28 (t, 2H), 4.72 ppm (m, 1H); FTIR (KBr pellet): $\tilde{\nu}$ = 3208, 2916, 2850, 1736, 1591, 1532, 1472, 1260, 1200 cm^{-1}; ESI-MS: *m/z*: 416.5 [$M^+ + H$].

C_{18}-thio-Glu ($C_{18}D_{37}$ chain): ^{1}H NMR (400 MHz): δ = 2.5–2.7 (m, 2H), 2.97 (t, 2H), 4.79 ppm (t, 1H); FTIR (KBr pellet): $\tilde{\nu}$ = 3200, 2190, 2088, 1733 cm^{-1}; ESI-MS: *m/z*: 453.76 [$M^+ + H$].

C_{18}-TE-Glu ($C_{18}H_{37}$ chain): ^{1}H NMR (400 MHz): δ = 0.88 (t, 3H), 1.28 (br m, 35H), 2.35 (m, 2H), 2.6 (t, 2H), 3.0 (q, 2H), 4.08 (m, 2H), 4.28 ppm (m, 1H); FTIR (KBr pellet): $\tilde{\nu}$ = 2919, 2853, 1736, 1726, 1660, 1467, 1208, 1135 cm^{-1}; ESI-MS: *m/z*: 444.5 [$M^+ + H$].

C_{18}-TE-Glu ($C_{18}D_{37}$ chain): ^{1}H NMR (400 MHz): δ = 1.27 (t, 3H), 2.2–2.35 (m, 2H), 2.59 (m, 2H), 3.0 (q, 2H), 4.7 ppm (t, 1H); FTIR (KBr pellet): $\tilde{\nu}$ = 2190s, 2088s, 1733, 1648s, 1208 cm^{-1}; ESI-MS: *m/z*: 481.86 [$M^+ + H$].

C_{18}-Glu-NCA ($C_{18}H_{37}$ chain): ^{1}H NMR (400 MHz): δ = 0.88 (t, 3H), 1.25 (br m, 32H), 2.1–2.3 (m, 2H), 2.55 (t, 2H), 4.09 (t, 2H), 4.37 (t, 1H), 6.22 ppm (s, 1H); FTIR (KBr pellet): $\tilde{\nu}$ = 3276, 2919, 2851, 1857, 1848, 1812, 1770, 1735, 1241, 1182, 933 cm^{-1}; ESI-MS: *m/z*: 414.52 [$M^- - H$].

C_{18}-Glu-NCA ($C_{18}D_{37}$ chain): ^{1}H NMR (400 MHz): δ = 2.1–2.3 (m, 2H), 2.62 (t, 2H), 4.45 (t, 1H), 6.28 ppm (s, 1H); FTIR (KBr pellet): $\tilde{\nu}$ = 3268, 2204, 2085, 1846, 1802, 1768, 1733, cm^{-1}; ESI-MS: *m/z*: 461.46 [$M^- - H$].

As catalysts, we used nickel acetate · 4 H_2O (Aldrich), I_2/KI prepared by dissolution of crystalline I_2 (1.9 g, 7.5 mmol; Merck) into an aqueous solution of KI (0.4 M, 60 mL) and $AgNO_3$ (Aldrich).

Sample preparation: The solutions (0.5 mM) of the amphiphile monomers were prepared in chloroform for C_{18}-TE-Lys, C_{18}-TE-Glu, and C_{18}-Glu-NCA, or in chloroform with 1% TFA for C_{18}-thio-Glu. The solutions were spread on water for a nominal molecular area (area of the trough divided by the total number of molecules contained in the spreading solution) of 35 Å^2, corresponding to ~70% monolayer coverage. The temperature of the water subphase was 20 °C, except for C_{18}-Glu-NCA where the water was cooled to 4 °C(or to close to 0 °C). Under these conditions, the surface pressure did not increase above 1 mN m^{-1}. GIXD measurements were performed after cooling to 4 °C and purging with cold helium. For the monolayers of C_{18}-TE-Lys, C_{18}-TE-Glu, and C_{18}-thio-Glu, the polycondensation reactions were initiated by addition of concentrated aqueous solutions of I_2/KI or $AgNO_3$ catalysts into the subphase beneath the monolayer to reach a final concentration of 1 mM and 5 mM, respectively. For the monolayers of C_{18}-Glu-NCA, the polymerization was initiated by addition of concentrated aqueous solutions of nickel acetate to reach a concentration of 5 mM. The reaction time was two to four hours.

MALDI-TOF MS: After the reaction, the monolayer films were compressed with the barrier and the material, observed by visual inspection, was collected from the liquid surface, transferred to a glass vial and dried under vacuum. Samples for the MALDI-TOF MS analysis were then prepared by dissolving the dry material in chloroform containing 1% trifluoroacetic acid. One microliter of this solution was deposited on top of a matrix deposit (1:1 v/v of dithranol solution in chloroform and NaI saturated solution in THF) on the instrument holder. The MALDI-TOF positive-ion mass spectra were obtained in reflector mode from two different instruments at the Weizmann Institute (Bruker Biflex 3) and at the University of Paris VI (Perceptive Biosystems, Voyager Elite), both equipped with a N_2 laser. External calibration of the mass spectra was achieved using calibrating peptide (Substance P, ACTH 8-39) in the studied mass range. Only singly charged ions, $[M+H]^+$, $[M+Na]^+$ and $[M+2Na-H]^+$ with the expected isotopic pattern, were observed. Other ions with the same isotopic pattern were often observed and shifted by $\Delta m/z$ of 4 units and 6 units and 113 units with respect to $[M+Na]^+$ and $[M+2Na-H]^+$, presumably resulting from the gas-phase reaction of these species or formation of an adduct with one trifluoroacetic acid ion (114 units). The nature of these ions is currently under investigation. Deuteration of the different compounds being not complete, but lying in the range 98.6% (C_{18}-TE-Glu), 97.9% (C_{18}-TE-Lys), a program was developed by using Visual Basic (V5.2) to derive the complex isotopic pattern of the oligopeptide species from that of the monomers comprising either protonated or perdeuterated hydrocarbon chains. In these experiments, the isotopic pattern for a given oligomeric species containing protonated and deuterated units and the mass precision (better than 0.1 unit) are sufficiently well defined to correctly assign the monomer composition of the various observed ions. Mass spectra resulted from a signal average of at least a few hundreds of laser shots in different spots of the target in order to get a reliable statistic about the ion peak. The good statistic is obtained when the isotopic distribution of an ion species corresponds to that expected from the calculation. Mass assignments were made using both *m/z* measurement and isotopic distribution (different from protonated and deuterated monomers). A good agreement was found on both instruments for the observed ions and their relative abundance.

We use the following notation code of the oligopeptide molecules: (*h*,*d*) designates a molecule comprising *h* *S*(deuterated) repeat units and *d* *R*(protonated) repeat units, with $n = h + d$, being the total number of repeat units. The relative abundance (*ra*) of each type of oligopeptide (*h*,*d*) is obtained by dividing the intensity of all the ions from a particular molecule to the total intensity of the ions from all the molecules of the same length, *n*. For example, the relative abundance of a tetra-peptide (4,0) composed of four *R*(protonated) chains, is calculated with Equation (1).

$$ra(4,0) = \text{intensity}(4,0)/\text{intensity}\{(4,0)+(3,1)+(2,2)+(1,3)+(0,4)\} \quad (1)$$

The relative abundance of the tetrapeptide (2,2) composed of two *R*(protonated) and two *S*(deuterated) chains is calculated with Equation (2).

$$ra(2,2) = \text{intensity}(2,2)/\text{intensity}\{(4,0)+(3,1)+(2,2)+(1,3)+(0,4)\} \quad (2)$$

A very similar ionization yield is expected for the (*h*,*d*) oligopeptides of the same length $n = h + d$, due to identical chemical properties. In addition, the very close masses of those compounds and the very close ion velocities in the TOF mass spectrometer allow to expect similar detection efficiency.[53] Thus the ion intensity of the different (*h*,*d*) oligopeptides are directly and reliably comparable.

The enhancement factors where calculated by dividing the relative abundance of any oligopeptide by the corresponding experimental values obtained for the C_{18}-thio-Glu system that was found experimentally to undergo an almost random polycondensation.

GIXD measurements: These were performed by using the liquid–surface diffractometer mounted at the BW1 synchrotron beamline at Hasylab, DESY, Hamburg. Details about the experimental technique and the instrument were reported elsewhere.[22] The measured GIXD patterns are represented as two-dimensional contour maps of the scattered intensity, $I(q_{xy}, q_z)$, as a function of the horizontal q_{xy} and vertical q_z components of the scattering vector. The unit cell dimensions of the 2D lattice are derived from the q_{xy} positions of the Bragg peaks. The full width at half maximum of the Bragg peaks (corrected for instrument resolution), FWHM(q_{xy}), gives an estimate of the crystalline coherence lengths $L_{hk} \approx 0.9(2\pi/\text{FWHM}(q_{xy}))$ associated with each *h*,*k* reflection. Bragg rod intensity profiles are the intensity distribution along q_z, $I(q_z)$, derived by integrating across the q_{xy} range for each of the Bragg peaks. The full width at half maximum of the Bragg rod intensity profiles, FWHM(q_z), gives a first estimate of the thickness $d \approx 0.9(2\pi/\text{FWHM}(q_z))$ of the 2D crystallites. More accurately, the intensity at a particular value of q_z in a Bragg rod is determined by the square of the molecular structure factor $|F_{h,k}(q_z)|^2$. The 2D packing arrangement is determined by performing X-ray structure factor calculations, using atomic coordinate molecular models constructed using the CERIUS^2 molecular package,[37] and rigid-body structure refinement, using the SHELX-97 program[38] adapted for 2D structures.

Acknowledgement

We thank the Israel-Science Foundation, The Petroleum Research Funds of the American Chemical Society, The Israel Ministry of Science, Culture and Sport, and the Danish Foundation for Natural Sciences for financial support. This work was supported by the IHP-Contract HPRI-CT-1999-00040/2001-00140 of the European Community. We are grateful to HASYLAB at DESY, Hamburg, for beam time at the BW1 beamline.

[1] W. A. Bonner, *Orig. Life Evol. Biosph.* **1991**, *21*, 59.
[2] L. E. Orgel, *Nature* **1992**, *358*, 203.

[3] P. Franck, W. A. Bonner, R. N. Zare in *Chemistry for the 21th Century*, (Eds.: E. Keinan, I. Schecter), Wiley-VCH, Weinheim, **2000**, pp. 175.
[4] J. Jacques, A. Collet, S. W. Wilen, *Enantiomers, Racemates and Resolutions*, Wiley, New York, **1981**.
[5] I. Weissbuch, R. Popovitz-Biro, L. Leiserowitz, M. Lahav in *Perspectives in Supramolecular Chemistry, vol. 1, The State of the Art - 100 Years of the The Lock-and-Key Principle*, (Ed.: J.-P. Behr), Wiley, New York, **1994**, pp. 173.
[6] D. K. Kondepudi, K. K. Asakura, *Acc. Chem. Res.* **2001**, *34*, 946.
[7] F. C. Frank, *Biochem. Biophys. Acta* **1953**, *11*, 459.
[8] V. Avetisov, V. Goldanski, *Proc. Natl. Acad. Sci. USA* **1996**, *93*, 11435.
[9] M. Bolli, R. Micura, A. Eschenmoser, *Chem. Biol.* **1997**, *4*, 309.
[10] J. S. Siegel, *Chirality*, **1998**, *10*, 24 – 27.
[11] A. Sagathelian, Y. Yokobyashi, K. Soltani, M. R. Ghadiri, *Nature* **2001**, *409*, 797.
[12] N. E. Blair, F. M. Dirbas, W. A. Bonner, *Tetrahydron* **1981**, *37*, 27.
[13] J. P. Ferris, A. R. H. Jr., R. Liu, L. E. Orgel, *Nature* **1996**, *381*, 59.
[14] B. L. Feringa, R. A. van Delden, *Angew. Chem.* **1999**, *111*, 3624 – 3645; *Angew. Chem. Int. Ed.* **1999**, *38*, 3418 – 3438.
[15] K. Soai, T. Shibata, I. Sato, *Acc. Chem. Res.* **2000**, *33*, 382.
[16] D. G. Blackmond, *Acc. Chem. Res.* **2000**, *33*, 402.
[17] M. Idelson, E. R. Blout, *J. Am. Chem. Soc.* **1958**, *80*, 2387 – 2393.
[18] R. D. Lundberg, P. Doty, *J. Am. Chem. Soc.* **1957**, *79*, 3961 – 3972.
[19] A. Brack, *Pure Appl. Chem.* **1993**, *65*, 1143.
[20] M. Blocher, T. Hitz, P. L. Luisi, *Helv. Chim. Acta* **2001**, *84*, 842.
[21] T. Hitz, M. Blocher, P. Walde, P. L. Luisi, *Macromolecules* **2001**, *34*, 2443.
[22] I. Kuzmenko, H. Rapaport, K. Kjaer, J. Als-Nielsen, I. Weissbuch, M. Lahav, L. Leiserowitz, *Chem. Rev.* **2001**, *101*, 1659.
[23] D. R. Day, H. Ringsdorf, *J. Polym. Sci., Polym. Lett. Ed.* **1978**, *16*, 205.
[24] F. H. Quina, D. G. Whitten, *J. Am. Chem. Soc.* **1977**, *99*, 877.
[25] D. A. Holden, H. Ringsdorf, M. Haubs, *J. Am. Chem. Soc.* **1984**, *106*, 4531.
[26] Y. Tanaka, K. Nakayama, S. Iigima, T. Shimizu, Y. Maitani, *Thin Solid Films* **1985**, *133*, 165.
[27] H. Koch, A. Laschewsky, H. Ringsdorf, K. Teng, *Makromol. Chem.* **1986**, *187*, 1843.
[28] A. Shibata, A. Oasa, Y. Hashimura, S. Yamashita, S. Ueno, T. Yamashita, *Langmuir* **1990**, *6*, 217 – 221.
[29] A. Shibata, Y. Hashimura, S. Yamashita, S. Ueno, T. Yamashita, *Langmuir* **1991**, *7*, 2261 – 2265.
[30] K. Fukuda, Y. Shibasaki, H. Nakahara, M. Liu, *Adv. Colloid Interface Sci.* **2000**, *87*, 113.
[31] H. Zepik, E. Shavit, M. Tang, T. R. Jensen, K. Kjaer, G. Bolbach, L. Leiserowitz, I. Weissbuch, M. Lahav, *Science* **2002**, *295*, 1266.
[32] Note that an inversion symmetry element, so prevalent in 3D crystals, is absent in the 2D counterpart since, at the air – water interface, amphiphilic molecules are perforce oriented with their hydrocarbon chains emerging into the air.
[33] M. Lahav, F. Laub, E. Gati, L. Leiserowitz, Z. Ludmer, *J. Am. Chem. Soc.* **1976**, *98*, 1620.
[34] I. Weissbuch, M. Berfeld, W. G. Bouwman, K. Kjaer, J. Als-Nielsen, M. Lahav, L. Leiserowitz, *J. Am. Chem. Soc.* **1997**, *119*, 933 – 942.
[35] I. Weissbuch, G. Bolbach, H. Zepik, E. Shavit, M. Tang, J. Frey, T. R. Jensen, K. Kjaer, L. Leiserowitz, M. Lahav, *J. Am. Chem. Soc.* **2002**, *124*, 9093.
[36] The measured Bragg rod $q_{xy} = 0.685\,\text{Å}^{-1}$ is very weak.
[37] CERIUS^2, Accelrys Inc., San Diego, CA, **1995**.
[38] G. M. Sheldrick, "SHELX97" Program for the Refinement of Crystal Structures, University of Göttingen, Germany, **1997**.
[39] Note that Figure 2a shows the measured and calculated Bragg rods of the three strong reflections. The other two observed Bragg rods (not shown) are very weak (< 5% of the strong reflections), the calculated Bragg rods of which are also very weak since their contribution arise primarily from the head group.
[40] I. Kuzmenko, V. M. Kaganer, L. Leiserowitz, *Langmuir* **1998**, *14*, 3882.
[41] The GIXD patterns measured from the enantiomerically pure (*S*)-C_{18}-thio-Glu 0.5 – 2.5 h after injection of the catalyst into the water subphase exhibited a gradual change to a single and very broad Bragg rod (not shown).
[42] L. Addadi, E. Gati, M. Lahav, L. Leiserowitz, *Israel J. Chem.* **1977**, *15*, 116.
[43] J. C. Sheehan, D. A. Johnson, *J. Am. Chem. Soc.* **1952**, *74*, 4726.
[44] L. Zang, J. P. Tam, *J. Am. Chem. Soc.* **1999**, *121*, 3311.
[45] Ag^+ ions, that are a good complexing agent for both N(amine) and S(ethyl) atoms, act as an efficient catalyst for the formation of amide bonds in cyclic oligopeptides.[44] The I_2/KI catalyst operates via the oxidation of the divalent S atom into the corresponding diiodo derivative that is a good leaving group.[43].
[46] I. Weissbuch, I. Kuzmenko, M. Vaida, S. Zait, L. Leiserowitz, M. Lahav, *Chem. Mater.* **1994**, *6*, 1258 – 1268.
[47] The self-assembly of non-racemic mixtures of γ-stearyl-glutamic acid into a racemic compound phase coexisting with an enantiomorphous phase was demonstrated by GIXD.
[48] Catalytic asymmetric processes displaying non-linear effects invoke differences in reactivity between homochiral and heterochiral dimeric species.[16,48].
[49] C. Girard, H. B. Kagan, *Angew. Chem.* **1998**, *110*, 3088—3127; *Angew. Chem. Int. Ed.* **1998**, *37*, 2922 – 2959.
[50] W. H. Daly, D. Poché, *Tetrahedron Lett.* **1988**, *29*, 5859.
[51] D. Wasserman, J. D. Garber, F. M. Meigs, US Patent 3,285,953, **1966**.
[52] R. Cricchio, M. Berti, G. Cietto, A. DePaoli, G. Tamborini, *Eur. J. Med. Chem.-Chimica Terapeutica* **1981**, *16*, 301.
[53] A. Brunelle, P. Chaurand, S. Della-Negra, Y. L. Beyec, E. Parilis, *Rapid Comm. Mass Spectrom.* **1997**, *11*, 353.

Received: September 30, 2002 [F4467]

  0947-6539/03/0908-1794 $ 20.00+.50/0